



UNIVERSITY OF
BATH

Gu, C., Wu, J. and Li, F. (2012) Reliability-based distribution network pricing. IEEE Transactions on Power Systems, 27 (3). pp. 1646-1655. ISSN 0885-8950

Link to official URL (if available):

<http://dx.doi.org/10.1109/TPWRS.2012.2187686>

2012 IEEE. Personal use of this material is permitted. Permission from IEEE must be obtained for all other users, including reprinting/republishing this material for advertising or promotional purposes, creating new collective works for resale or redistribution to servers or lists, or reuse of any copyrighted components of this work in other works

Opus: University of Bath Online Publication Store

<http://opus.bath.ac.uk/>

This version is made available in accordance with publisher policies.
Please cite only the published version using the reference above.

See <http://opus.bath.ac.uk/> for usage policies.

Please scroll down to view the document.

Reliability based Distribution Network Pricing

Chenghong Gu, *Student Member, IEEE*, Jianzhong Wu, *Member, IEEE*, and Furong Li, *Senior Member, IEEE*

Abstract— As a tool for network operators to recover network investment costs from network users as well as to provide forward-looking economic signals, distribution network pricing models are also expected to identify and recover investment costs related to maintaining network security. The existing models reflect network security by determining the maximum allowed contingency flow along each component through implementing deterministic contingency analysis. They fail to consider two reliability cost drivers: i) reliability levels of network components and, ii) interruption tolerance levels at different nodes.

For the first time, this paper proposes a novel distribution network pricing model to reflect two key reliability cost drivers: i) the nodal unreliability tolerance mandated by security standards, which is linked to the customer size at the node and ii) the stochastic nature of component reliability that reflects differing failure rates of network components. By combining the two factors, the new reliability based pricing model is able to recognize the impact on network investment from network components' reliability in addition to their distance and the degree of utilization. The concept is firstly demonstrated on three small networks: a single circuit system, a parallel-circuit system and a meshed system. The applicability of the new pricing approach to practical systems is then illustrated on a practical distribution network in the UK system.

Index Terms-- Network pricing, reliability, unreliability tolerance, failure rate, mean time to repair, tolerable loss of load.

I. INTRODUCTION

THE deregulation in the power industry has significantly increased the competition and promoted the efficiency of the sector throughout the world. It has however also imposed great uncertainties on power network planning and operation. In the competitive environment, network operators have no control over the sizes and sites of potential network users, but can use economic incentives to influence their decision makings. The use-of-system (UoS) charges are one of the most important forms of incentives, which are the charges levied on generators, large industrial consumers, and suppliers for their use of the network [1-4]. It is desirable that the UoS pricing methodologies can recover the costs of network investment, operation, and maintenance from network users in a cost-reflective way such that they are incentivized to choose the most economic sizes and locations so as to minimize network investment.

In line with network planning security standards [5-7], all networks are designed to be able to withstand credible contingencies that would affect the supply reliability. Table I gives part of the UK distribution network planning standards, Engineering Recommendation P2/6 [6], outlining the required security levels against differing sizes of demand groups. As shown by the table, the planning standards require smaller user groups to be secured against N-1 contingencies and larger groups against N-2 or even high orders of contingencies. In addition, the standards also specify the allowed interruption durations and amounts for each customer group, but it is still based deterministic criteria, assuming all components having the same probability of failure rate.

TABLE I
PART OF THE ENGINEERING RECOMMENDATION P2/6 IN THE UK [6]

Class	Group	First circuit outage	Second circuit outage
A	$\leq 1\text{MW}$	In repair time: group demand	Nil
B	$\leq 1\text{MW}$ $\leq 12\text{MW}$	(a) within 3 hours: group minus 1MW (b) In repair time: group	Nil
C	$\leq 12\text{MW}$ $\leq 60\text{MW}$	(a) within 15 minutes: smaller of (group minus 12MW); and 2/3 of group (b) within 3 hours: group	Nil
D	$\leq 60\text{MW}$ $\leq 300\text{MW}$	(a) immediately: group minus up to 12 MW (b) within 3 hours: group	(c) within 3 hours: for group greater than 100MW: smaller of (group minus 100MW); and 1/3 group (d) within time to restore arranged outage: group
...

Due to aging, human misoperation, bad weather, or intentional attacks, all components are not 100% reliable and they would fail at certain rates according to historic experience [8]. Maintaining a certain level of network reliability is crucial to both customers and operators. For customers, they might suffer huge monetary loss due to supply interruption, and for operators, they would be penalized by regulators for not providing the mandated reliability levels. Basically, there are two ways to improve network security: i) to restore the failed components in shorter time; ii) to ensure sufficient redundancies in systems such that when some components fail, the supply will not be interrupted. It is usually neither possible nor economical to guarantee 100% reliability due to the high operation and investment costs [9]. That is why security standards usually allow a certain level of load interruption for a period of time for particular customer groups [6].

Chenghong Gu and Furong Li are with the Department of Electronic and Electrical Engineering, University of Bath, Bath BA2 7AY, U.K. (e-mail: c.gu@bath.ac.uk; f.li@bath.ac.uk). Jianzhong Wu is with the Institute of Energy, School of Engineering, Cardiff University, UK (e-mail: wuj5@cardiff.ac.uk)

Network pricing as a means to recover the investment costs from network users should also reflect users' contribution to the costs needed in maintaining an appropriate level of reliability or security of supply [10-14]. Substantial research has been conducted on pricing with network security/reliability, but the majority of the work focuses on allocating the embedded network cost in transmission systems [15-18]. These approaches allocate the embedded costs based on marginal reliability margin and capacity share between normal and abnormal conditions. None of them can reflect the costs of future reinforcement and consequently are unable to influence the locations and sizes of the future generation and demand. Another disadvantage associated with the transmission charging approaches is that they do not consider differing interruption tolerance for customers.

The charging methodologies at the distribution level are less advanced. Prior to 2007, there was no locational distribution charging methodologies and the fixed costs are allocated based on yardstick approaches with differing sophistication [19, 20]. The increasing distributed generators (DG) need locational signals at the distribution level to guide their sizes and sites [21]. The UK is the first country introducing locational network charges at the distribution level. The Long-run Incremental Cost (LRIC)- utilized at its Extra High Voltage (EHV) distribution networks seeks to reflect the impact on future investment in networks as a result of a generation injection or a load withdrawal at each study node [22, 23]. The model also considers network security when identifying reinforcement costs and calculating charges [24]. It assigns each component with a contingency factor, defined as the ratio of the component's maximum contingency flow under N-1 or N-2 contingencies over its normal flow and the component available capacity is then scaled down accordingly with the factor [10]. The maximum contingency flow is the flow along a component under its most serious contingency; the most serious contingency is the contingency event that gives rise to the largest increase in the component's power flow. The other charging model used at EHV distribution networks - Forward Cost Pricing (FCP) - runs network contingency analysis to determine the volume of components' rated capacity needed to be reserved for the worst contingency events [24, 25]. The two approaches are still based on two assumptions: i) all components have the same failure rates and, ii) all nodes connected with customers have no supply interruption allowance. These assumptions overestimate the impacts of network security on long-term investment and generate less cost-reflective network charges.

A novel network pricing model for higher voltage distribution networks is proposed to integrate the stochastic features of component reliability and allowed nodal supply interruptions. Due to the complexity of reliability calculation [26, 27], it is very hard to directly include it in network charging. An alternative method is to use analytical approaches to simplify the calculations [28, 29]. Firstly, the allowed nodal load loss and the allowed interruption duration are combined together to form nodal Expected Energy Not

Supply (EENS) to reflect the nodal tolerance to supply interruptions. Then, the calculated EENS together with a component's Mean Time to Repair (MTTR) and annual Failure Rate (FR) are used to form the nodal tolerable loss of load (TL_{oL}). The new method curtails the nodal TL_{oL} supported by each component when determining its maximum flow in contingencies that define its future reinforcement. The flow is then translated into its reinforcement horizon and the impacts of nodal injections or withdraws are reflected by recognizing the change in the component reinforcement horizon. The model is able to recognize the impact on network investment from customer unreliability allowance and components reliability levels. The proposed model is demonstrated on a two-busbar notional network and an actual distribution system taken from the U.K. network. Sensitivity analysis is also conducted to investigate the impacts of component reliability and nodal unreliability tolerance on the nodal charges.

The rest of this paper is organized as: Section II introduces the deterministic and reliability based network reinforcement methodologies. In section III, the impact of network reliability on component reinforcement horizons in three typical networks are studied. Section IV introduces the normal case reinforcement horizon calculation and section V reports the framework of the proposed model. Sections VI and VII employ two systems to demonstrate the proposed method. Section VIII presents a short discussion of using commercial reliability package to facilitate the application of the proposed approach. Section IX concludes this paper.

II. DETERMINISTIC AND RELIABILITY-BASED NETWORK REINFORCEMENT

Methodologies used for identifying future investment costs in a network charging model can be generally divided into two categories: deterministic criteria based and reliability based. The deterministic approaches reinforce a network when it can no longer securely supply its demand under network contingencies as required by security standards. By contrast, the reliability based planning reinforces a network when the required reliability level at the customer end is violated as a result of demand/generation growth.

The comparison of the two types of principles is carried out on the notional two-busbar system given in Fig.1, where a demand group P is supported by two identical circuits.

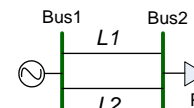


Fig.1. Two-circuit radial network.

A. Deterministic Approach

Suppose that the security standards require that the demand group should be secured against N-1 contingencies. When L1 fails, L2 is sufficient as long as it can still accommodate the demand group, but should be reinforced immediately if it is unable to do so. Therefore, the time taking the initial demand

to grow to L2's full capacity is given by

$$RC = P_0 \cdot (1 + r)^n \quad (1)$$

where RC is L2's rated capacity, P_0 is the initial demand size, r is the chosen load growth rate and n is L2's reinforcement time horizon.

B. Reliability-based Approach

The reliability-based approaches acknowledge that it is neither possible nor economical for network operators to guarantee 100% supply reliability, but a certain degree of supply interruption at a node, i.e. nodal EENS, is acceptable. This nodal allowance will in turn allow circuits, which support the nodal demand, to have some degree of tolerable power curtailment. The level of the tolerance is dictated by the failed component's failure rate and MTTR and the nodal EENS. By combining the three factors, the nodal EENS is translated into branch tolerable loss of load of the working components, i.e. the flow along them that can be curtailed when the other components fail, given by

$$TLoL = \frac{EENS}{MTTR \cdot FR} \quad (2)$$

where, $EENS$ is the product of the amount of load can be interrupted at a node and its duration. MTTR and FR are the failed component's mean time to repair and failure rate.

This formula translates nodal unreliability tolerance and component reliability into the level of load that can be interrupted during network contingencies. Smaller MTTR indicates that it takes less time to restore the failed component, and thus for a given EENS tolerance, the working circuit could withstand larger load loss and give rise to larger TLoL. The same goes to FR.

The reliability based planning reinforces the network when the TLoL at a busbar overtakes the tolerable threshold specified in security standards. In Fig.1, L2's reinforcement horizon is thereby derived with (3) when L1 fails.

$$TLoL = P_0 \cdot (1 + r)^n - RC \quad (3)$$

where, $TLoL$ is the tolerable loss of load at busbar 2 determined by its allowed EENS and L1's MTTR and FR.

C. The Difference

The difference between the two approaches can be shown by comparing (1) and (3). The difference is that (3) includes the nodal TLoL in determining component reinforcement horizons, but (1) does not. Equation (1) is to gauge the time taking the demand to grow to L2's capacity when L1 fails, it is based on two assumptions: i) L1's failure rate is 1, i.e. it definitely fails at some point in the studied period; ii) no load loss is tolerable at busbar 2. By contrast, (3) integrates the reliability of L1 and the tolerable nodal load loss, and allows that part of load curtailed when determining L2's reinforcement horizon. Therefore, it can better reflect the actual network planning practice. As there will be additional TLoL in a component, the reinforcement time horizon from the reliability based approach is always bigger than that from deterministic based approach. The magnitude of the difference depends on three factors: the nodal EENS, the failed

component's MTTR and FR.

III. COMPONENT REINFORCEMENT IN CONTINGENCIES

This section calculates component investment horizons with the inclusion of component reliability and nodal unreliability tolerance for three typical networks: a single-circuit network, a parallel-circuit network, and a meshed network in two scenarios: with and without a nodal demand increment.

A. Single-circuit Case

For the single-circuit network given in Fig. 2, the tolerable supply interruption at busbar 2 is assumed to be EENS₀.

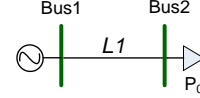


Fig.2. A single-circuit network.

The outage of L1 will interrupt the total demand P_0 at busbar 2, but if P_0 is smaller than the threshold size specified in security standards required for N-1 contingency security level there is no need to reinforce L1 (for purpose of demonstration, the case that L1 is under repair or maintenance is not considered). As P_0 grows at a given rate, the demand group size will reach the threshold at some point in the future and by that time L1 should be reinforced. The time taking P_0 to grow to the threshold is identified with

$$TLoL = P_0 \cdot (1 + r)^n \quad (4)$$

This formula can be rewritten by submitting (2) into it

$$\frac{EENS_0}{MTTR_1 \cdot FR_1} = P_0 \cdot (1 + r)^n \quad (5)$$

where, $MTTR_1$ and FR_1 are L1's MTTR and FR, and r is the predicted load growth rate

Rearranging and taking logarithm of (5) produces (6), which is L1's reinforcement horizon without any injections.

$$n = \frac{\log\left(\frac{EENS_0}{MTTR_1 \cdot FR_1}\right) - \log(P_0)}{\log(1 + r)} \quad (6)$$

A demand increment at busbar 2 increases the load loss when L1 fails and consequently it brings forward the circuit's reinforcement horizon. If the nodal unreliability tolerance level is to be maintained, i.e. $EENS_0$ is the same before and after the nodal increment, the new horizon can be determined by

$$\frac{EENS_0}{MTTR_1 \cdot FR_1} = (P_0 + \Delta P) \cdot (1 + r)^{n_{new}} \quad (7)$$

where, ΔP is the extra flow along L1 due to the increment.

Rearranging it produces

$$n_{new} = \frac{\log\left(\frac{EENS_0}{MTTR_1 \cdot FR_1}\right) - \log(P_0 + \Delta P)}{\log(1 + r)} \quad (8)$$

B. Parallel-circuit Case

For the two parallel-circuit network given in Fig.1, it is assumed that the two circuits are identical. The reliability

based approach is demonstrated on L1's reinforcement calculation. Suppose that L2's MTTR is $MTTR_2$, FR is FR_2 and rated capacity is RC_2 , and the nodal tolerable EENS is $EENS_0$. If L2 fails, L1's reinforcement is triggered when the demand grows to a level that exceeds the branch loss of load tolerance. Based on the analysis in Section II, L1's investment horizon can be calculated by submitting (2) into (3) and taking logarithm of it, producing

$$n = \frac{\log\left(\frac{EENS_0}{MTTR_2 \cdot FR_2} + RC\right) - \log(P_0)}{\log(1+r)} \quad (9)$$

When a new injection comes to busbar 2, L1's new investment horizon can be calculated by replacing P_0 in (9) with $(P_0 + \Delta P)$

$$n_{new} = \frac{\log\left(\frac{EENS_0}{MTTR_2 \cdot FR_2} + RC\right) - \log(P_0 + \Delta P)}{\log(1+r)} \quad (10)$$

where, ΔP is the extra contingency flow along L1 due to the injection when L2 fails.

L2's reinforcement horizons with and without an injection can be calculated in the same way.

C. Meshed Network Case

For a simple meshed network in Fig.3, it is assumed that if L1 fails, it will cause the maximum contingency flow along L2 and L3, i.e., their future reinforcement requirement is defined by the demand increase when L1 fails. The tolerable EENS at busbars 2 and 3 are $EENS_1$ and $EENS_2$ respectively

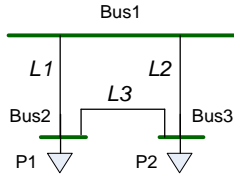


Fig.3. A simple meshed network.

Similar to the previous two cases, L2's reinforcement horizon in the contingency event is determined by the time taking the circuit power flow to grow from the current level to its rated capacity plus the amount TLoL that could be curtailed at busbars 2 and 3, given by

$$TLoL_1 + TLoL_2 = (P_1 + P_2) \cdot (1+r)^n - RC_2 \quad (11)$$

where, P_1 and P_2 are the demand at busbars 2 and 3, $TLoL_1$ and $TLoL_2$ are their respective loss of load tolerance, and RC_2 is L2's rated capacity.

Rearranging (11) and submitting (2) into it produces

$$n = \frac{\log\left(RC_2 + \frac{EENS_1 + EENS_2}{MTTR_1 \cdot FR_1}\right) - \log(P_1 + P_2)}{\log(1+r)} \quad (12)$$

When a load increment is experienced at either bus 2 or bus 3, it will change L2's investment horizon. The new investment horizon can be obtained by replacing $(P_1 + P_2)$ in (12) with $(P_1 + P_2 + \Delta P)$

$$n_{new} = \frac{\log\left(RC_2 + \frac{EENS_1 + EENS_2}{MTTR_1 \cdot FR_1}\right) - \log(P_1 + P_2 + \Delta P)}{\log(1+r)} \quad (13)$$

where, ΔP is L2's power flow increment due to the nodal injection when L1 fails.

L3's reinforcement horizon can be identified in the same way as L2, given by

$$TLoL_1 = P_1 \cdot (1+r)^n - RC_3 \quad (14)$$

Rearranging it gives

$$n = \frac{\log\left(\frac{EENS_1}{MTTR_1 \cdot FR_1} + RC_3\right) - \log(P_1)}{\log(1+r)} \quad (15)$$

Similarly, its new reinforcement horizon with an injection at busbar 2 is

$$n_{new} = \frac{\log\left(\frac{EENS_1}{MTTR_1 \cdot FR_1} + RC_3\right) - \log(P_1 + \Delta P)}{\log(1+r)} \quad (16)$$

Where, ΔP is L3's power flow increment when L1 fails.

It should be pointed out that the TLoL that can be curtailed during network contingencies in determining a component's reinforcement horizon is the sum of all the nodal tolerable load loss the component supports. For example, in this meshed network, the total curtailed TLoL in calculating L2's horizon is the sum of the tolerable nodal load loss at busbars 2 and 3.

IV. COMPONENT REINFORCEMENT UNDER NORMAL CONDITIONS

Component's reinforcement can be triggered by demand growth in either normal or contingency conditions; the smaller one in the two conditions defines the actual horizon. Similar to (1), under normal conditions the reinforcement horizon of a component without any injections is

$$n = \frac{\log(RC) - \log(P_i)}{\log(1+r)} \quad (17)$$

where, RC is the component's rated capacity and P_i is its normal case flow.

Its new reinforcement horizon with an injection can be obtained by replacing P_i in (17) with $(P_i + \Delta P)$

$$n_{new} = \frac{\log(RC) - \log(P_i + \Delta P)}{\log(1+r)} \quad (18)$$

where, ΔP is the circuit's incremental power flow under the normal conditions.

V. FRAMEWORK OF THE NEW NETWORK PRICING

The core of the new charging model is to: i) determine the impact of nodal power perturbation on components' reinforcement horizons when considering the two key reliability cost drivers, and ii) translate the impact into the change in the present value of components' future reinforcement. The implementation steps of the new model are summarized as follows.

A. Branch Tolerable Load Loss and Maximum Contingency Flow

The prerequisite task of analyzing nodal injection on network components is: i) to investigate how nodal TLoL affects branches' flows, defined as branch TLoL, and ii) the maximum contingency flow along each component with the branch TLoL curtailed. In each contingency, power flow is first executed and then sensitivity analysis is used to determine the relationship between nodal injections and branch flows, i.e. how a nodal increment would affect branch flows [12]. It is therefore possible to determine components' flows with the nodal TLoL at each busbar curtailed. By repeating this in all contingency events, the maximum contingency flows along components can be determined.

If a network component fails, the associated nodal TLoL can be calculated with (2), where MTTR and FR are the failed component's reliability parameters. The tolerable nodal EENS is obtained by multiplying nodal tolerable load loss with the allowed outage duration. If more than one component fails simultaneously or one component fails when the other is under maintenance, the equivalent MTTR and FR should be calculated by combining the reliability parameters of the all out of service components using reliability theory [8].

B. Component's Original Horizon without Injections

Components' original horizons under normal case are determined by: i) running power flow analysis to calculate components' power flows; ii) feeding the obtained results into (7) to determine the investment horizons. The maximum contingency flows of all components calculated in step (A) are submitted into (6), (9), (12), or (15), according to the network configurations, to calculate their contingency case reinforcement horizons. The smaller values from the normal and contingency cases are chosen as their actual original reinforcement horizons.

C. Component's New Horizon with Injections

Add an injection at each study busbar and then run power flow analysis to calculate components' new reinforcement horizons under normal case with (18). Under network contingency, a nodal injection is applied to every studied busbar to run contingency analysis to calculate all components' maximum contingency flows. Then, since we have determined the correlation between components' flows and the nodal injections in each contingency in step (A), it is therefore easy to determine their new maximum contingency flows with the nodal TLoL curtailed. The new maximum contingency branch flows are then fed into (8), (10), (13) or (16) to determine their new reinforcement horizons. Similar to Step (B), the smaller time horizons are chosen as their actual reinforcement horizons.

D. Unit Price

When the original and new reinforcement horizons of a component are identified, its unit incremental cost for each study busbar can be assessed by calculating the changes in its present value of future reinforcement. The present value of the

future reinforcement of the component is

$$PV = \frac{Cost}{(1+d)^n} \quad (19)$$

where, d is discount rate and n is its original investment horizon obtained in Step (B) and $Cost$ is its investment cost.

The change in the present value of future investment as a result of an injection is

$$\Delta PV = Cost \cdot \left(\frac{1}{(1+d)^{n_{new}}} - \frac{1}{(1+d)^n} \right) \quad (20)$$

where, n_{new} is the component new reinforcement horizon determined in Step (C),

The incremental cost of the component is the annuitized change in the present value of future investment

$$\Delta IC = \Delta PV \cdot AnnuityFactor \quad (21)$$

The nodal incremental cost for a node is the accumulation of the incremental costs over all components supporting the node over the size of the nodal injection

$$LRIC = \frac{\sum IC}{\Delta PI} \quad (22)$$

where, ΔPI is the size of the nodal injection.

E. Flowchart

The proposed network pricing is also shown in the flowchart in Fig.4, illustrating how to take into account the two reliability cost drivers in a network pricing model.

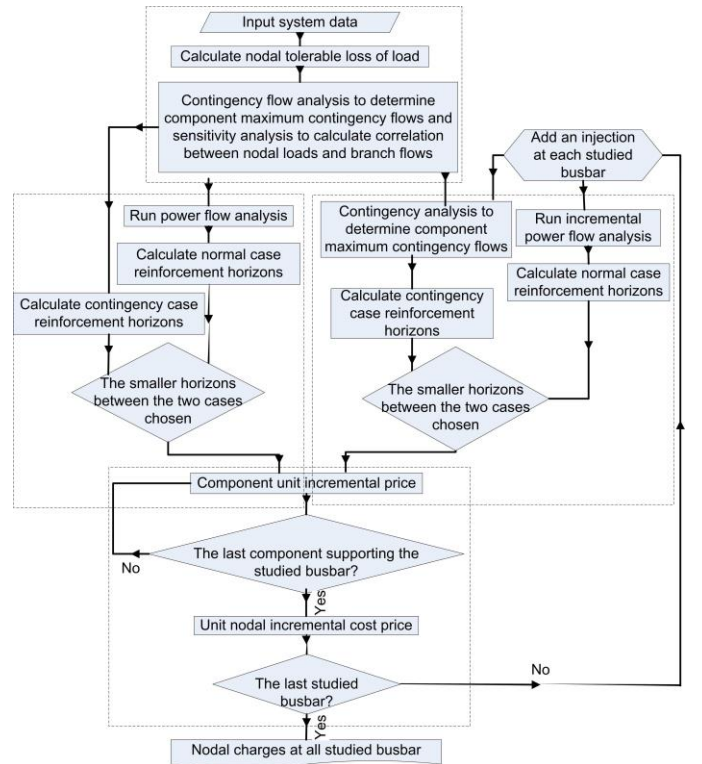


Fig.4. Flowchart of the proposed method

The proposed method respects both component reliability (in terms of failure rate and mean time to repair) and nodal tolerable supply interruption (in terms of allowed nodal load loss and the allowed duration) when determining components

reinforcement horizons. Although the concept is demonstrated on notional systems, it can be equally applied to large-scale practical systems following the steps given above and shown in Fig.4. The underlying reliability information and security analyses can be processed by any professional software, such as PSS/E [30]. The approach does need additional information in addition to basic network information, such as line and transform impedance and costs. Besides, utilities need to supply their components' reliability information and suppliers need to supply their customer sizes. In Section VII, we will demonstrate our approach on an actual distribution system area from the UK network.

VI. DEMONSTRATION ON A SMALL SYSTEM WITH DC FLOW

In this section, the proposed approach is demonstrated and compared with the original LRIC model on the simple network given in Fig.3, using DC load flow. D1 and D2 are assumed to be 10 MW and 20MW respectively, each with a growth rate of 1.0%. For simplicity purposes, the three circuits are assumed to be identical, and their parameters are presented in Table II.

TABLE II
CIRCUIT PARAMETERS

Capacity (MW)	Cost (£)	MTTR (hour/time)	FR (hour/year)	Failure period (hour/year)
45	1,596,700	7.5	0.5	3.75

According to P2/6, the allowed nodal load loss is supposed to be 1MW within 3 hours for busbar 1 and 3MW within 3 hours for busbar 2, which produces a tolerable EENS of 3MWh at busbar 1 and 9MWh at busbar 2.

A. Charge Calculation

Table III outlines the base case states of the three circuits.

TABLE III
RESULTS OF THE THREE-BUSBAR SYSTEM

Circuit No.	L1	L2	L3
Normal power flow (MW)	13.33	16.67	3.33
Maximum contingency flow (MW)	30	30	20
Contingency factor	2.25	1.8	6.0
The most serious contingency event	L2 out	L1 out	L2 out

As seen, the maximum contingency flows along L1 and L3 are caused by L2's failure and L2's maximum contingency flow appears when L1 fails. By comparing the normal and contingency cases, it is noted that the three circuits' reinforcement is triggered by the demand growth in contingency situations. When L2 fails, the sensitivity at busbar 2 to the flow along L1 and the sensitivity at busbar 3 to the flows along L1 and L3 are all 1.0, i.e. 1MW nodal injection at each busbar will cause 1 MW flow increment along the circuits.

For assisting understanding, we take the case of calculating the nodal charge for busbar 3 as an example. When no injection is connected to the busbar, the three circuits' maximum flows are 30MW, 30MW and 20MW respectively, as given in Table III. The TLoL at the two busbars is

calculated by dividing 3MWh and 9MWh with the product of MTTR (7.5h/time) and FR (0.5time/ry), producing 0.8MW and 2.4MW respectively. Since, the sensitivity is 1.0, the reduction demand of 0.8MW and 2.4MW will cause the same branch reduction in the same amount. By feeding these results into (12) or (15), we obtain the three circuits' reinforcement horizons, which are 47.65yrs, 47.65yrs and 88.40yrs respectively shown in Table IV.

When 1MW injection is applied to busbar 3, the three circuits' maximum flows are still driven by the failures of L2 L1 and L2 respectively, but the values become to 31MW, 31MW and 21MW. When the nodal TLoL is curtailed, we can therefore calculate their new reinforcement horizons with (13) or (16), which produces 44.36yrs for L1, 44.36yrs for L2 and 83.50yrs for L3. By submitting their old and new reinforcement horizons into (20), we can easily determine the incremental costs from the three circuits for the customer at busbar 3 given in Table V. The summation of the three incremental costs divided by the injection size is the actual incremental charge for busbar 3, which is 2548.05 £/MW/yr.

TABLE IV
HORIZONS OF THE THREE CIRCUITS IN CONTINGENCIES (YR)

Injection location	L1	L2	L3
No injection	47.65	47.65	88.40
Bus 2	44.36	44.36	88.40
Bus 3	44.36	44.36	83.50

TABLE V
RESULTS OF THE THREE-BUSBAR SYSTEM (£/MW/YR)

	Cost from L1	Cost from L2	Cost from L3	Total charge
Bus 2	1211.17	1211.17	0.00	2422.34
Bus 3	1211.17	1211.17	125.70	2548.05

Similarly, when an injection is applied to busbar 2, the reinforcement horizons of the three circuits and consequently the incremental costs can be calculated in the same way. The results are given in Table IV and Table V respectively. The final charge is 2422.34 £/MW/yr for busbar 2.

B. Comparison with the Original LRIC Model

The original LRIC model [11] also accounts for supply security but in a rather simplistic approach. It assumes all circuits having the same MTTR and FR, and the nodal tolerance to supply interruption is zero. As such, it restricts the amount of flow through the circuits under the normal condition. The maximum allowed power flow for a circuit under contingency condition is determined by reshaping their rated capacity with their contingency factors given in Table III. As a result, the maximum allowed power flows along L1, L2 and L3 under the normal condition are 20MW, 25MW and 7.5MW respectively despite that the three circuits have an identical rated capacity. Table VI provides their reinforcement horizons calculated with and without injections on the basis of the maximum allowed capacity.

Table VI
REINFORCEMENT HORIZONS OF THE THREE CIRCUITS WITHOUT EENS
TOLERANCE (YR)

Injection location	L1	L2	L3
No injection	40.75	40.75	81.50
Bus 2	35.85	38.76	92.09
Bus 3	38.27	36.81	71.92

Compared with the results from the proposed approach in Table IV, most future investment horizons are reduced, implying the investments required come earlier. This is because the original LRIC does not consider circuits' reliability level but assumes they will fail at some point over the year, nor the TLoL at each load busbar. One exception is that when an injection is connected to busbar 2, L3's investment horizon is deferred to 92.09 yrs, as the injection reduces its flow.

TABLE VII
RESULTS OF THE THREE-BUSBAR SYSTEM (£/MW/YR)

	Cost from L1	Cost from L2	Cost from L3	Total charge
Bus 2	3019.59	1108.24	-260.76	3867.07
Bus 3	1404.94	2347.28	460.41	4212.63

Table VII outlines the incremental cost of each component and the final charges for each node. As seen, most incremental costs are higher than those from the proposed approach in Table VI. One exception is that an injection at busbar 2 can gain a reward of £260.76MW/yr for using L3. Actually, the injection has no impact on L3's future reinforcement, as the injection has no impact on its maximum contingency flow, so it should not be rewarded. The proposed model can capture this point, generating no reward for users at busbar 2 for using L3. The final charges are 3.67.07£/MW/yr for busbar 2 and 4212.63 £/MW/yr for busbar 3; both are bigger than those from the proposed model.

VII. DEMONSTRATION ON A PRACTICAL NETWORK

This section carries out the comparison of the two approaches on a practical Grid Supply Point (GSP) area taken from the UK network depicted in Fig.5.

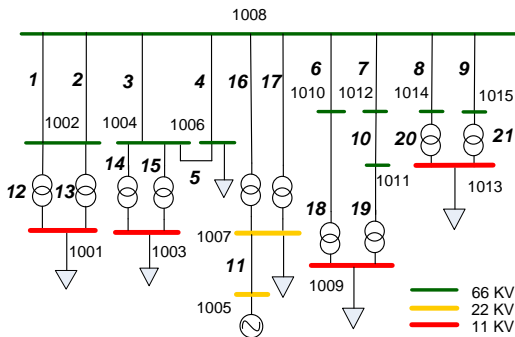


Fig. 5. A Grid Supply Point (GSP) area test system.

The discount rate and load growth rate are chosen as 6.9% and 1.0% respectively. For the purpose of simplicity and ease

in explanation, all branches are supposed to have the same repair time of 4 hour/time and failure rate of 0.5time/year. The combination of the two factors produces a failure period of 2 hour/year. For each component, as the MTTR and FR have the same effect on the TLoL according to (2), the following analysis only focuses on the impact incurred by FR.

Table VIII outlines all load busbars' allowed load loss and the calculated tolerable EENS. Busbar 1001 has the smallest EENS of 3.5MWh. Busbar 1003's EENS is the biggest, 4.5MWh, followed by other four busbars that have the same EENS. The EENS combined with the MTTR and FR of a failed component is utilized to calculate the nodal TLoL in each network contingency.

TABLE VIII
NODAL RELIABILITY INDICES

Busbar	1001	1003	1006	1007	1009	1013
Allowed nodal load loss (MW)	7.0	9.0	2.0	8.0	2.0	2.0
Duration (hour)	0.5	0.5	2.0	0.5	2.0	2.0
EENS (MWh)	3.5	4.5	4.0	4.0	4.0	4.0

A. Low Utilization Level Case

This part carries out the calculations at system base loading level in three different scenarios, in which the GSP area is assumed to have different reliability levels:

- Scenario 1: use base nodal reliability level in Table VIII;
- Scenario 2: increase nodal reliability level by decreasing nodal allowed load loss down to the half of the original values, causing the nodal tolerable EENS and TLoL halved;
- Scenario 3: increase nodal reliability levels by decreasing assets' FRs to the half of the original values, causing the TLoL doubled.

Table IX provides the calculated nodal charges under the three scenarios as well as those from the original LRIC model. Compared with scenarios 1 and 3, scenario 2 produces the highest charges for all 6 load busbars: the highest charge is 25.74£/kW/yr at busbar 1003 and the lowest is 0.21 £/kW/yr at busbar 1009. This is because lower allowed load loss means that less demand can be interrupted in contingencies and hence more asset spare capacity should be reserved to accommodate the potential extra contingency flows and thus reduces asset maximum available capacity. Scenario 3 produces the lowest charges in all scenarios, as smaller asset FR indicates that they are less likely to fail and therefore for a given EENS level, less spare capacity needs to be reserved for contingencies.

TABLE IX
NODAL CHARGE COMPARISON IN FOUR SCENARIOS (£/kW/YR)

Busbar	1001	1003	1006	1007	1009	1013
Scenario 1: base case	4.08	20.22	16.66	1.46	0.18	0.91
Scenario 2: lower LoL	4.90	25.74	21.29	1.79	0.21	1.26
Scenario 3: smaller FR	2.88	12.80	10.46	0.98	0.13	0.50
Original approach	5.59	32.59	26.80	2.14	0.24	1.71

Although both scenarios 2 and 3 have improved nodal reliability levels, the calculated charges vary greatly. The reason is that scenario 2 produces smaller TLoL, but in scenario 3, the TLoL is enlarged because component FR is reduced. By contrast, the original LRIC model generates the highest charges for all load busbars, as it assumes that component's rated capacity is reduced by the contingency factors and thus a tiny injection would dramatically bring forward the investment. The highest charge also appears at busbar 1003, counted as 32.59 £/kW/yr, and the lowest is 0.24 £/kW/yr for busbar 1009.

From another aspect, the charges from the proposed approach in all three scenarios maintain the relativity pattern from the original model: bus 1003's charge is the highest, followed by bus 1006 and the charge at bus 1013 is the lowest.

B. High Utilization Level Case

In this part, the comparison is carried out in the same three scenarios previously utilized but with higher component utilization levels. The calculated results are given in Table X.

TABLE X
NODAL CHARGE COMPARISON (£/kW/YR)

Busbar	1001	1003	1006	1007	1009	1013
Scenario 1: base case	8.44	41.99	34.08	2.95	0.41	1.85
Scenario 2: lower LoL	10.13	53.45	43.56	3.62	0.49	2.56
Scenario 3: smaller FR	5.96	26.59	21.40	1.99	0.29	1.01
Original approach	11.53	67.70	54.95	4.28	0.52	3.49

Compared with results in Table IX, charges for all studied busbars here grow dramatically. Particularly, the highest charge is found as 67.70 £/kW/yr at busbar 1003 from the original model, followed by 53.45 £/kW/yr generated by scenario 3. The high charges are due to the increased component loading levels, which greatly bring forward their reinforcement horizons. On the other hand, the relative sizes in charges are still maintained as observed.

C. Impact of TLoL and FR

This part investigates the influence of two major factors that affect nodal charges: nodal unreliability tolerance and asset FR on the nodal charges. For simplicity purposes, only busbar 1003 is analyzed.

Fig.6 demonstrates the charge at busbar 1003, varying with respect to the decrease in its nodal unreliability tolerance, i.e. the amount of allowed load loss. The results from the proposed model are depicted with the solid line and those produced by the original model are represented by the dashed line. As seen, when the allowed load loss is around 30% of the load at busbar 1003, the charge from the new model is about 25.5 £/kW/yr, which increases gradually with the decline in the tolerance. It reaches approximately 33 £/kW/yr when the allowed load loss is zero. The charge from the original model, by contrast, persists at 32.59 £/kW/yr, as it does not consider any nodal TLoL.

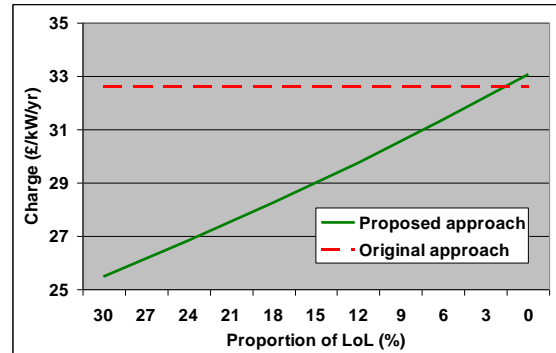


Fig.6. Charge variation with respect to the allowed LoL.

It is noted that when the allowed load loss percentage is close to zero, the two lines cross at a point, and beyond it, the charge from the proposed model exceeds that from the original model. It is because the original model considers that an injection at 1003 can defer L5's investment horizon and therefore it produces a reward for busbar 1003 for using L5. By contrast, the proposed model produces no incremental cost or reward for the busbar from L5.

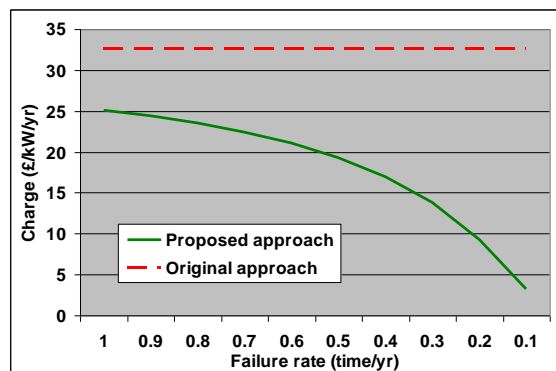


Fig.7. Charge variation with respect to failure rate.

In Fig.7, the impact of component reliability on busbar 1003's charge is presented. Obviously, the charge from the new model decreases gradually with the decline in 1003's supporting components' FRs. When they are 1.0 time/yr, the charge is approximately 25 £/kW/yr, which decreases steadily to merely about 4 £/kW/yr when the FRs are 0.1 time/yr. The reason is that when the FRs are small, the components rarely fail and hence less of their capacity needs to be reserved for catering for contingencies. In the extreme cases that all components' failure rates are zero, i.e. they never fail, there is no need to reserve component capacity to accommodate contingency. Under such context, the charges only depend on components' rated capacity, load growth rate, and system loading conditions.

As demonstrated, nodal charges are brought down by considering nodal unreliability tolerance and component reliability, the degree of which depends on the allowed load loss size and component reliability levels. Bigger unreliability tolerance and more reliable components tend to generate low charges, and vice versa. For network operators, although increasing component reliability levels, achieved by reducing

failure rate and restored time, can increase nodal reliability levels and thereafter reduce nodal charges, the costs to deliver the actions could be enormous. For network users, they would see lower charges if they can tolerate greater load loss, but the loss due to energy interruption could increase in turn. Whatever decisions they make, the tradeoff between gains and costs should be carefully examined.

VIII. DISCUSSION

In network pricing, it is important to respect the investment costs for maintaining network security and reliability. Generally, there are two types of methodologies used to calculate network reliability: Simulation based and analytical approach based [28, 29, 31, 32] and this paper uses analytical approaches in integrating reliability into network pricing. In order to fully reflect reliability related investment costs, the proposed approach has to run contingency analysis to examine how nodal injections would affect components' reinforcement under contingency situations. The existing distribution system analysis software packages, such as PSS/E, Digsilent, and ETAP, have the ability to run network contingency and reliability analysis [30, 33]. Further, through the use of Python, extensive reliability and contingency analyses can be automated under the professional software environment such as PSS/E. The obtained results can be easily fed into this new pricing model to calculate nodal charges.

IX. CONCLUSION

In order to reflect the cost of network security in network charging, this paper, for the first time, incorporates nodal unreliability tolerance and the supply component's reliability into a distribution network charging model. It works by reflecting how a component's failure rate and mean time to repair would affect its ability to deliver energy to customers, and how customers' tolerance to supply interruption under contingencies will impact the component's time to reinforce. Based on the analysis in the paper, the following observations can be obtained:

- The proposed model overcomes two disadvantages of the existing pricing models: i) relying on deterministic criteria to reflect the cost of network security; and ii) unable to respect the nodal unreliability tolerance. It works by incorporating both factors into assessing the impact of a nodal perturbation on assets' investment horizons. The new model can better reflect the actual network planning practice and the stochastic features of network failures.
- Component reliability, allowed nodal load loss and the failure duration are the three major factors influencing nodal reliability. The new model reduces the nodal charges by considering them: more reliable components and larger unreliability tolerance lead to smaller charges, and vice versa.
- The new model maintains the merits of the original LRIC model of being able to produce locational and cost-reflective charges to influence prospective users' behaviors

to maximize the utilization of the existing networks, particularly those with higher reliability level and shorter time to repair.

- One problem with the new model is that it would need substantial computational effort to analyze network contingencies for large-scale systems. We ran the proposed model on a practical EHV distribution network in the UK, comprising 1,898 busbars: it took the original LRIC method approximately 30 minutes to calculate charges for all load busbars but the proposed approach about 27 hours. Although it is a 50 fold increase in time, network charges are calculated on an annual basis and thus such an increase in running time is affordable by network operators to better reflect their investment decisions. Besides, the advance in computational techniques can benefit the application of the proposed method.

Future research needs to investigate the correlation between nodal charges, the costs of different reliability improvement strategies, and how customers might respond to the locational charges so as to find the economic equilibrium for both network operators and users. Additionally, the benefits in network investment deferral brought about by renewable generators are not considered in distribution network pricing in the UK currently, due to their output intermittency. Future work can also be conducted to examine how it would be more cost-effective to charge them, respecting the impact that they not only can bring forward network reinforcement but also might defer the needed network investment.

REFERENCES

- [1] D. Shirmohammadi, X. V. Filho, B. Gorenstin *et al.*, "Some fundamental, technical concepts about cost based transmission pricing," *Power Systems, IEEE Transactions on*, vol. 11, no. 2, pp. 1002-1008, 1996.
- [2] Z. Jing, X. Duan, F. Wen *et al.*, "Review of transmission fixed costs allocation methods," *Power Engineering Society General Meeting, 2003, IEEE*. p. 2592 Vol. 4.
- [3] D. Shirmohammadi, C. Rajagopalan, E. R. Alward *et al.*, "Cost of transmission transactions: an introduction," *Power Systems, IEEE Transactions on*, vol. 6, no. 4, pp. 1546-1560, 1991.
- [4] A. Zobian, and M. D. Ilic, "Unbundling of transmission and ancillary services. II. Cost-based pricing framework," *Power Systems, IEEE Transactions on*, vol. 12, no. 2, pp. 549-558, 1997.
- [5] G. SQSS. "Security and Quality of Supply Standard," http://www.nationalgrid.com/NR/rdonlyres/FBB211AF-D4AA-45D0-9224-7BB87DE366C1/15460/GB_SQSS_V1.pdf.
- [6] E. E. N. Association), "Engineering Recommendation P2/6," 2006.
- [7] K. R. W. Bell, N. Green, D. Nicol *et al.*, "Security criteria for planning and operation in the new GB market," in *Cigre*, 2006, pp. 1-8.
- [8] R. Billinton, and R. N. Allan, *Reliability of Evaluation of power systems*, Second ed., 1996.
- [9] V. Udo, S. K. Agarwal, A. Vojdani *et al.*, "Balancing cost and reliability: a quantitative study at Atlantic Electric," *Power Systems, IEEE Transactions on*, vol. 12, no. 3, pp. 1103-1111, 1997.
- [10] R. J. Kaye, F. F. Wu, and P. Varaiya, "Pricing for system security [power tariffs]," *Power Systems, IEEE Transactions on*, vol. 10, no. 2, pp. 575-583, 1995.
- [11] H. Y. Heng, F. Li, and X. Wang, "Charging for Network Security Based on Long-Run Incremental Cost Pricing," *Power Systems, IEEE Transactions on*, vol. 24, no. 4, pp. 1686-1693, 2009.
- [12] C. Gu, and F. Li, "Long-Run Marginal Cost Pricing Based on Analytical Method for Revenue Reconciliation," *Power Systems, IEEE Transactions on*, vol. 26, no. 1, pp. 103-110, 2011.

- [13] P. D. C. Wijayatung, B. J. Cory, and M. J. Short, "Security and revenue reconciliation in optimal transmission pricing," *Generation, Transmission and Distribution, IEE Proceedings*, vol. 146, no. 4, pp. 355-359, 1999.
- [14] C. W. Yu, and A. K. David, "Pricing transmission services in the context of industry deregulation," *Power Systems, IEEE Transactions on*, vol. 12, no. 1, pp. 503-510, 1997.
- [15] J. Yu, and A. D. Patton, "Transmission use charges including reliability costs," *Power Engineering Society Winter Meeting, 2000. IEEE*. pp. 866-871.
- [16] H. Monsef, and M. Jaefari, "Transmission cost allocation based on use of reliability margin under contingency conditions," *Generation, Transmission & Distribution, IET*, vol. 3, no. 6, pp. 574-585, 2009.
- [17] E. L. Silva, S. E. C. Mesa, and M. Morozowski, "Transmission access pricing to wheeling transactions: a reliability based approach," *Power Systems, IEEE Transactions on*, vol. 13, no. 4, pp. 1481-1486, 1998.
- [18] K. Hyungchul, and C. Singh, "Consideration of the reliability benefits in pricing transmission services," *Power Engineering Society Winter Meeting, 2001. IEEE*. pp. 1232-1237.
- [19] J. W. M. Lima, J. C. C. Noronha, H. Arango *et al.*, "Distribution pricing based on yardstick regulation," *Power Systems, IEEE Transactions on*, vol. 17, no. 1, pp. 198-204, 2002.
- [20] P. M. DeOliveira-DeJesus, M. T. PoncedoLeao, J. M. Yusta *et al.*, "Uniform Marginal Pricing for the Remuneration of Distribution Networks," *Power Systems, IEEE Transactions on*, vol. 20, no. 3, pp. 1302-1310, 2005.
- [21] P. M. Sotkiewicz, and J. M. Vignolo, "Allocation of fixed costs in distribution networks with distributed generation," *Power Systems, IEEE Transactions on*, vol. 21, no. 2, pp. 639-652, 2006.
- [22] F. Li, and D. L. Tolley, "Long-Run Incremental Cost Pricing Based on Unused Capacity," *Power Systems, IEEE Transactions on*, vol. 22, no. 4, pp. 1683-1689, 2007.
- [23] F. Li, N. P. Padhy, J. Wang *et al.*, "Cost-Benefit Reflective Distribution Charging Methodology," *Power Systems, IEEE Transactions on*, vol. 23, no. 1, pp. 58-64, 2008.
- [24] W. A. "FCP methodology implementation and guidance notes."
- [25] Frontier. "Review of distribution use of system charging methodology," <http://www.eon-uk.com/downloads/FrontierEconomicsG3DUoSChargesFinal250308.pdf>.
- [26] J. D. McCalley, V. Vittal, and N. Abi-Samra, "An overview of risk based security assessment," *Power Engineering Society Summer Meeting, 1999. IEEE*. pp. 173-178 vol.1.
- [27] J. McCalley, S. Asgarpoor, L. Bertling *et al.*, "Probabilistic security assessment for power system operations," *Power Engineering Society General Meeting, 2004. IEEE*. pp. 212-220 Vol.1.
- [28] G. Kjolle, and K. Sand, "RELRAD-an analytical approach for distribution system reliability assessment," *Power Delivery, IEEE Transactions on*, vol. 7, no. 2, pp. 809-814, 1992.
- [29] R. Billinton, and P. Wang, "Distribution system reliability cost/worth analysis using analytical and sequential simulation techniques," *Power Systems, IEEE Transactions on*, vol. 13, no. 4, pp. 1245-1250, 1998.
- [30] SIEMENS, "PSS/E User Manual," <http://www.energy.siemens.com/us/en/services/power-transmission-distribution/power-technologies-international/software-solutions/pss-e.htm>, 2011.
- [31] R. Billinton, and W. Peng, "Teaching distribution system reliability evaluation using Monte Carlo simulation," *Power Systems, IEEE Transactions on*, vol. 14, no. 2, pp. 397-403, 1999.
- [32] W. Zhuding, F. Shokooh, and Q. Jun, "An efficient algorithm for assessing reliability indexes of general distribution systems," *Power Systems, IEEE Transactions on*, vol. 17, no. 3, pp. 608-614, 2002.
- [33] DigSILENT, "DigSILENT Solutions PowerFactory Software," *Power and Energy Magazine, IEEE*, vol. 4, no. 5, pp. 3-3, 2006.

Jianzhong Wu (M'06) is a Lecturer in Institute of Energy, Cardiff School of Engineering. Prior to this, he was a Research Fellow at the University of Manchester from 2006 to 2008. His research activities are focused on Energy Infrastructure and Smart Grids. He is a member of IEEE, IET and ACM.

Furong Li (M'00, SM'09) was born in Shannxi province, China. She received the B.Eng. degree in electrical engineering from Hohai University, Nanjing, China, in 1990 and the Ph.D. degree from Liverpool John Moores University, Liverpool, U.K., in 1997. She then took up a lectureship with Department of Electronic & Electrical Engineering, University of Bath, where she is a Professor in the Power and Energy Systems Group at the University of Bath, Bath, U.K. Her major research interest is in the area of power system planning, analysis, and power system economics.

Chenghong Gu (S'09) was born in Anhui province, China. He received his Bachelor degree and Master degree in electrical engineering from Shanghai University of Electric Power and Shanghai Jiao Tong University, Shanghai, China, in 2003 and 2007 respectively. In 2010, he obtained his PhD from University of Bath, U.K. Now, he is working as a KTA fellow in the Dept. of Electronic & Electrical Eng., University of Bath. His major research is in the area of power system planning, economics and smart grid.